Decoherence recuperating fast environmental dynamics

2010 J. Phys. A: Math. Theor. 43 055309

(http://iopscience.iop.org/1751-8121/43/5/055309)

IOP PUBLISHING JOURNAL OF PHYSICS A: MATHEMATICAL AND THEORETICAL

J. Phys. A: Math. Theor. **43** (2010) 055309 (19pp) doi:10.1088/1751-8113/43/5/055309

Decoherence recuperating fast environmental dynamics

Murat Çetinbaş

Laboratory for Advanced Spectroscopy and Imaging Research, 4D LABS and Department of Chemistry, Simon Fraser University, Burnaby, British Columbia, V5A 1S6, Canada

E-mail: cetinbas@sfu.ca

Received 15 July 2009, in final form 20 November 2009
Published 14 January 2010
Online at stacks.iop.org/JPhysA/43/055309

Abstract

We examine the exact internal decoherence dynamics of a qubit in an isolated Josephson charge-qubit quantum computer in the presence of one- and two-body static internal imperfections. By help of open system dynamics quantifiers, i.e. purity, fidelity, covariance and Loschmidt echo, we distinguish between non-unitary and unitary components of internal decoherence dynamics and show that the non-unitary component consists of two processes: system-environment entanglement and incoherence. Our results indicate that the incoherence process is the major source of internal decoherence rather than system-environment entanglement. We find that strong one-body intra–environmental interactions, which generate fast environmental dynamics, result in a rapid suppression of decoherence induced by both system–environment entanglement and incoherence processes. We explain the mechanisms of suppression of decoherence for these two processes and discuss our results.

PACS numbers: 03.65.−w, 05.30.−d, 03.65.Yz, 03.67.Lx

(Some figures in this article are in colour only in the electronic version)

1. Introduction

Decoherence [1–3] caused by an external environment, surrounding a quantum computer (QC) core, is not the only factor hindering a QC's performance [4]: even when a QC core is completely isolated from its surrounding external environment [6], coherent dynamics of qubits within an isolated QC core is not guaranteed due to internal decoherence, dissipation and coherent shifts emerging from two–body static residual interactions and imperfections among qubits [7–10]. Isolated QCs [6] with static internal imperfections are prototypical examples of self-interacting—and possibly chaotic—complex finite environments for which exact quantum dynamics can readily be obtained on a classical computer. Exact dynamical results of

such studies can be very informative not only in elucidating the underlying mechanism of decoherence dynamics induced by complex environments but also in development of more effective error-correcting strategies for quantum computing [4, 5]. Recent studies of decoherence [7–11] reported two noteworthy effects, which are of particular importance to the performance of a QC in the presence of static internal imperfections. The first effect is the suppression of decoherence by chaotic environmental interactions [7–11]. The importance of this effect is that one can in principle tame a QC core with chaos to avoid decoherence [7–10]. Hence, a deliberately induced chaos may be used as an error-correcting strategy when the implementation of chaos-generating interactions is feasible. The second effect is destructive large unitary error arising from environment-induced coherent shifts (i.e. Lamb or Stark shift-like effects) [7–10]. These effects, even though unitary, impose serious limitations on the performance of quantum gates, and the bath chaos is not a very effective way to tackle the error of unitary type emerging from these shifts. In fact, the bath chaos in some instances amplifies such unitary error [7–10].

While recent studies [7–10] identified environment-induced coherent shifts as a potential source of unitary error, the existence of internal decoherence dynamics emerging from a non-unitary manifestation of these unitary shifts has not been appreciated. Residual qubit–qubit interactions mix the ideal (i.e. uncoupled) computational states of qubits. The mixing generates an internal decoherence mechanism, which in general consists of two distinct processes: system–environment entanglement (SEE) and incoherence. SEE process gives rise to entanglement-induced decoherence (EID) as a result of non-local correlations established between states of a qubit and its surrounding nearby qubit environment. The incoherence process brings about incoherence-induced decoherence (IID) via randomization of phase and even populations of a qubit's state. In a previous study [12], we distinguished between these two processes and showed that SEE can be nullified when an environment evolves in a decoherence–free subspace [13–16]. This condition allows us to drive the Kraus decomposition [17] of incoherence dynamics, which governs an exact equation of motion for an open quantum system when the incoherence process is the only source of decoherence [12].

The present study is concerned with manifestations of the above effects by non-chaotic environments. By exact numerical simulations and the Kraus decomposition of incoherence dynamics calculations [12], we investigate a spin–spin-bath model [18] designed to simulate an open system dynamics of a qubit in a many-qubit isolated Josephson charge-qubit QC [19–21] in the presence of one- and two-body static internal imperfections. By help of the open system dynamics quantifiers, i.e. purity, fidelity, covariance and Loschmidt echo, we analyze our exact numerical and the Kraus decomposition results separately. This novel approach allows us to distinguish the non-unitary component of open system dynamics from that of the unitary component and shows that the non-unitary component, responsible for internal qubit decoherence, is generated by both SEE and incoherence processes. We find that the major source of qubit decoherence stems from the incoherence process rather than SEE. We also find that strong one-body intra-bath interactions, which render a fast internal environmental dynamics, cause a rapid reduction of SEE, which in turn results in a fast diminution of not only EID but also IID. An interesting aspect of our study which may be contrary to some expectations is that we observe the suppression of decoherence as well as environment-induced large unitary error for a non-chaotic bath. In a number of previous studies [7–11], these effects have been attributed to the existence of two-body intra-bath interactions and thus to the chaotic bath dynamics. The fact that we observe the same effects in the opposite limit suggests that these effects are not truly intrinsic to the chaotic baths or baths with two-body intra-bath interactions.

The organization of this paper is as follows. In section 2 the mathematical details of our study are given: we define Hamiltonians and initial conditions, summarize our exact numerical

approach, review basics of incoherence dynamics and give numerical parameters used in our calculations. We summarize open system dynamics quantifiers in section 3, and report our results for these quantifiers in section 4. We discuss our results in section 5 and conclude our study in section 6.

2. The model

Residual qubit–qubit interactions emerging in a many-qubit QC core generate an unavoidable internal decoherence mechanism for the ideal computational states of qubits [7–10]. As a result, even though an external decoherence time, with respect to a macroscopic external environment surrounding a QC core, is so long that the QC core can be considered as an isolated closed system [6], qubits within such an isolated QC core experience their own nearby microscopic environments—thus are open quantum systems—and are subject to internal decoherence dynamics [7–10].

To investigate the internal decoherence dynamics of a qubit in an isolated QC core in the presence of one- and two-body static internal imperfections, we regard an isolated QC core as a two-component system, i.e. a central qubit is the subsystem and the rest of the isolated QC is the environment. Both the central qubit and its environment evolve unitarily in the absence of residual qubit–qubit interactions. However, once these interactions are in effect, the central qubit interacts with its nearby qubit environment and thus unitary quantum dynamics no longer holds. Any deviation from the unitary quantum dynamics is an error source for the central qubit. These deviations can be non-unitary, e.g. decoherence and dissipation, and also be unitary, e.g. environment-induced coherent shifts. Non-unitary deviations may originate from SEE or the incoherence process alone or both. Once the exact quantum dynamics of the isolated QC is known, the reduced density operator of the central qubit can be obtained and the origin, as well as the extent of these deviations, can be estimated by the help of open system dynamics quantifiers. This is the approach to be pursued in our study.

2.1. Hamiltonians

We consider the isolated QC core as a bipartite closed system, represented by the total Hamiltonian of the form

$$\hat{H} = \hat{H}_S + \hat{H}_B + \hat{S}\hat{B}, \tag{1}$$

where $\hat{H}_S$ is the system Hamiltonian of the central qubit:

$$\hat{H}_S = -\tfrac{1}{2} B_0^z \hat{\sigma}_z^{(0)} - \tfrac{1}{2} B_0^x \hat{\sigma}_x^{(0)}, \tag{2}$$

$\hat{H}_B$ is the bath Hamiltonian, representing the rest of the QC core:

$$\hat{H}_B = -\frac{1}{2}\sum_{i=1}^{N}\left(B_i^z \hat{\sigma}_z^{(i)} + B_i^x \hat{\sigma}_x^{(i)}\right) + \sum_{i=1}^{N-1}\sum_{j=i+1}^{N} J_x^{i,j} \hat{\sigma}_x^{(i)} \hat{\sigma}_x^{(j)}, \tag{3}$$

and $\hat{S}\hat{B}$ is the coupling operator, mediating interactions between the system $\hat{S}$ (i.e. the central qubit) and the bath $\hat{B}$ (i.e. the rest of the QC) degrees of freedom:

$$\hat{S}\hat{B} = \hat{\sigma}_{x/z}^{(0)} \hat{\Sigma}_{x/z}, \qquad \text{where} \quad \hat{\Sigma}_{x/z} = \sum_{i=1}^{N} \lambda_i \hat{\sigma}_{x/z}^{(i)}. \tag{4}$$

Here x/z means x or z. Hence, we consider two different types of coupling operator: bit-flip errors are generated by xx-type coupling and phase errors are generated by zz-type

coupling. In our notation, $\hat{\sigma}^{i}_{x/z}$ are the standard Pauli spin-1/2 operators where the central qubit is labeled with zero while the bath qubits are labeled with $i = 1, \ldots, N$ where N is the total number of bath qubits. To model one- and two-body qubit imperfections, we follow previous studies [6–10]. We assume that all qubits except the central qubit are subject to a static noise. We sample one-qubit parameters randomly and uniformly from the distributions $B^{z}_{i} \in \left[B^{z}_{c} - \delta_{z}/2, B^{z}_{c} + \delta_{z}/2\right]$ and $B^{x}_{i} \in \left[B^{x}_{c} - \delta_{x}/2, B^{x}_{c} + \delta_{x}/2\right]$. Here B^{x}_{c} and B^{z}_{c} are the centers of the distributions, and the detuning parameters $\delta_{x/z}$ are always set to $\delta_{x/z} = 0.4B^{x/z}_{c}$. Residual system-bath and intra-bath interactions are also randomly and uniformly sampled via the distributions $\lambda_{i} \in [-\lambda, \lambda]$ and $J^{i,j}_{x} \in [-J_{x}, J_{x}]$, respectively.

Solid state QCs inherit a variety of interactions to couple qubits; qubit–qubit residual interactions of xx-, yy-, zz- and xy-types may all be potential error generators for a particular QC architecture. In addition, the presence of impurities in a QC core may also lead to different error generators than those aforementioned. One-qubit imperfections are due to different energy spacing of qubits. Such imperfections emerge unavoidably especially for the manufactured qubits for which the reproducibility of identical qubits with the same energy spacing can be hard to achieve. In our study we employ xx- and zz-type couplings as error generators. Since these error generators do not commute, they allow us to explore different dynamical regimes of decoherence. Nevertheless, the distributions and the allowed imperfections used in our study should still be considered as an idealization, since the nature as well as the magnitude of imperfections would possibly be intrinsic to the actual experimental set-up and conditions.

2.2. Initial conditions and exact numerical approach

We assume that the system and bath states are initially uncorrelated:

$$\hat{\rho}(0) = \hat{\rho}_{S}(0) \otimes \hat{\rho}_{B}(0), \tag{5}$$

where the initial system state is a pure state:

$$\hat{\rho}_{S}(0) = |\psi(0)\rangle\langle\psi(0)| \qquad \text{with} \qquad |\psi(0)\rangle = (|0\rangle + |1\rangle)/\sqrt{2}, \tag{6}$$

and the initial bath state is of a Gibbsian form:

$$\hat{\rho}_{B}(0) = \sum_{n=1}^{2^{N}} p_{n}|n\rangle\langle n| \qquad \text{and} \qquad p_{n} = \exp\{-\beta E_{n}\} \Big/ \sum_{m=1}^{2^{N}} \exp\{-\beta E_{m}\}, \tag{7}$$

where p_{n} are the bath populations, $\beta = 1/k_{B}T$ is the inverse bath temperature, k_{B} is the Boltzmann constant and $\hat{H}_{B}|n\rangle = E_{n}|n\rangle$ are the exact eigenvalues and eigenvectors of the bath Hamiltonian.

The exact time evolution of the total density operator is obtained as a solution of Liouville–von Neumann equation:

$$\hat{\rho}(t) = \hat{U}(t)\hat{\rho}(0)\hat{U}^{\dagger}(t) \qquad \text{with} \qquad \hat{U}(t) = \exp\{-(\mathrm{i}/\hbar)\hat{H}t\}, \tag{8}$$

which is valid for all temperatures. However, since we are interested in the low temperature limit, relevant to the charge-qubit QC proposal [19–21], the above sum in (7) can be truncated as

$$\hat{\rho}_{B}(0) = \sum_{n=1}^{M} p_{n}|n\rangle\langle n| \qquad \text{and} \qquad p_{n} = \exp\{-\beta E_{n}\} \Big/ \sum_{m=1}^{M} \exp\{-\beta E_{m}\}, \tag{9}$$

where M represents the maximum number of populated bath states at the low temperature limit, i.e $M \ll 2^{N}$. As a rule of thumb, M must be chosen so that the states with $M + 1$ and higher are unoccupied for a given bath temperature.

In what follows, the exact quantum dynamics of the reduced density is obtained by tracing over the bath degree of freedom:

$$\hat{\rho}_S(t) = \sum_{n=1}^{M} p_n \,\mathrm{Tr}_B\{|\Psi_n(t)\rangle\langle\Psi_n(t)|\}, \tag{10}$$

where $|\Psi_n(t)\rangle = \hat{U}(t)|\Psi_n(0)\rangle$ are solutions to the Schrödinger equation for all initial conditions of the form $|\Psi_n(0)\rangle = |\psi(0)\rangle \otimes |n\rangle$.

2.3. Kraus decomposition of incoherence dynamics

The exact time evolution of the reduced density (10) can equivalently be expressed as an operator sum representation:

$$\hat{\rho}_S(t) = \sum_{n=1}^{M}\sum_{m=1}^{2^N} \hat{\mathcal{K}}_{m,n}(t)\hat{\rho}_S(0)\hat{\mathcal{K}}^{\dagger}_{m,n}(t) \qquad \text{where} \quad \hat{\mathcal{K}}_{m,n}(t) = \sqrt{p_n}\langle m|\hat{U}(t)|n\rangle. \tag{11}$$

Here $\hat{\mathcal{K}}_{m,n}(t)$ are the Kraus operators [17]. Equation (11) is valid for a general decoherence scenario in which a quantum subsystem may be subject to both SEE and incoherence processes. In a recent investigation [12], we have distinguished between these two processes and showed that SEE—and consequently EID—can be avoided when an environment evolves in a decoherence-free subspace [13–16]. Our decoherence-free environment condition[1] led us to the Kraus decomposition of incoherence dynamics [12]:

$$\hat{\rho}_S(t) = \sum_{n=1}^{M} \hat{\mathcal{K}}_{n,n}(t)\hat{\rho}_S(0)\hat{\mathcal{K}}^{\dagger}_{n,n}(t) \quad \text{where} \quad \hat{\mathcal{K}}_{n,n}(t) = \sqrt{p_n}\exp\{-(\mathrm{i}/\hbar)(\hat{H}_S + \hat{S}b^n)t\}, \tag{12}$$

where $b^n = \langle n|\hat{B}|n\rangle$ are the diagonal matrix elements of the bath coupling operator. In the course of open system evolution, non-local correlations established between states of a quantum subsystem and its environment led to the SEE process, which in turn results in EID in the subsystem. When a subsystem undergoes EID dynamics, the off-diagonal matrix elements of the bath coupling operator $b^{m,n} = \langle m|\hat{B}|n\rangle$ are non-zero, as is the case in equations (10) and (11). Under certain conditions, which we discuss in section 3.2, the dynamics of an environment evolves independently from the subsystem, i.e. in a decoherence-free fashion. Therefore, the non-local correlations generating SEE cannot be established and the incoherence dynamics emerges as the only source of decoherence.

Incoherence process originates from environment-induced coherent quantum fluctuations, in the course of which the free system Hamiltonian is shifted as $\hat{H}_S \to \hat{H}^n_S = \hat{H}_S + \hat{S}b^n$ for each populated bath state $|n\rangle$ of the canonical bath density $\hat{\rho}_B(0)$. Each shifted system Hamiltonian $\hat{H}^n_S$ then changes the coherent probability amplitude of a subsystem's state by a slightly different magnitude. The convex combination of coherent probability amplitudes results in destructive interferences, which induce the non-unitary incoherence process. In a sense, the incoherence process is a non-unitary manifestation of unitary quantum fluctuations. It is noteworthy that the incoherence process is unitary for a pure environment state, such

[1] Our decoherence-free environment condition slightly differs from the condition used in the Hamiltonian formulation of decoherence-free subspaces (DFSs) [13–15] in that we do not assume a degenerate set of eigenstates spanning a DFS. In this regard, our condition is equivalent to Zurek's definition of DFSs in terms of pointer states that are known to be immune to decoherence [16]. Details can be found in [12].

as when the bath temperature is absolute zero. In this case, the only effect induced by an environment is a coherent shift given by

$$\hat{\rho}_S(t) = \hat{\mathcal{K}}(t)\hat{\rho}_S(0)\hat{\mathcal{K}}^\dagger(t) \qquad \text{where} \quad \hat{\mathcal{K}}(t) = \exp\{-(\mathrm{i}/\hbar)(\hat{H}_S + \hat{S}b^{n=1})t\}, \tag{13}$$

where $n = 1$ stands for the ground state of bath.

To investigate how a fast environmental dynamics recuperates qubit coherence, we obtain both the exact decoherence dynamics (EDD) given by equation (10) and the incoherence dynamics (ID) predicted by the Kraus decomposition (12). The EDD comprises two non-unitary processes, i.e. SEE and incoherence. But the Kraus decomposition (12) is only exact for a quantum subsystem undergoing the absolute incoherence process, that is, the decoherence process in the absence of SEE. Nevertheless, the Kraus decomposition (12) can be used to estimate the extent of the incoherence process in a general decoherence dynamics. Hence, by a comparison between open system dynamics quantifiers, calculated separately for the EDD and ID, one can not only estimate the extent of decoherence caused by SEE and incoherence processes but also determine the relative importance of these processes. Distinguishing between these two processes may also help one focus on a specific source of decoherence that may be more readily corrected by currently available [4, 5] or specifically tailored error correction schemes.

The explicit form of Kraus operators governing ID renders possible to obtain analytic solution of reduced density for a large class of system–environment models. In our study the ID that the central qubit undergoes is governed by the Kraus operators

$$\hat{\mathcal{K}}_{n,n}(t) = \sqrt{p_n}\exp\left\{\frac{\mathrm{i}}{2\hbar}\left(B_0^z\hat{\sigma}_z^{(0)} + B_0^x\hat{\sigma}_x^{(0)} - 2b_{x/z}^n\hat{\sigma}_{x/z}^{(0)}\right)t\right\}, \tag{14}$$

where the diagonal matrix elements $b_{x/z}^n = \langle n|\hat{\Sigma}_{x/z}|n\rangle$ are calculated by using the exact eigenstates $|n\rangle$ of the bath Hamiltonian for all different cases, i.e. system–bath couplings given in equation (4) and bath configurations summarized in the next section. The time evolution of the density matrix elements of the central qubit is given by

$$\hat{\rho}_S(t) = \sum_{n=1}^{M} p_n \begin{pmatrix} |c_+^n(t)|^2 & c_+^n(t)[c_-^n(t)]^* \\ c_-^n(t)[c_+^n(t)]^* & |c_-^n(t)|^2 \end{pmatrix}, \tag{15}$$

where for the xx-type coupling,

$$c_\pm^n(t) = \frac{\sqrt{2}}{2}\left[\cos\left(\frac{\beta_x^n}{2\hbar}t\right) \pm \mathrm{i}\frac{\left(B_0^z \pm B_x^n\right)}{\beta_x^n}\sin\left(\frac{\beta_x^n}{2\hbar}t\right)\right], \tag{16}$$

$$\beta_x^n = \sqrt{B_0^{z\,2} + B_x^{n\,2}} \qquad \text{and} \qquad B_x^n = B_0^x - 2b_x^n \tag{17}$$

and for the zz-type coupling,

$$c_\pm^n(t) = \frac{\sqrt{2}}{2}\left[\cos\left(\frac{\beta_z^n}{2\hbar}t\right) \pm \mathrm{i}\frac{\left(B_z^n \pm B_0^x\right)}{\beta_z^n}\sin\left(\frac{\beta_z^n}{2\hbar}t\right)\right], \tag{18}$$

$$\beta_z^n = \sqrt{B_0^{x\,2} + B_z^{n\,2}} \qquad \text{and} \qquad B_z^n = B_0^z - 2b_z^n. \tag{19}$$

2.4. Choice of numerical parameters

Josephson QC architectures [19–21] are ideal systems to study internal decoherence dynamics due to their extremely long external decoherence time $\sim 10^{-4}$ s, which in principle allows $\sim 10^6$ single qubit operation. Our numerical analysis is based on a recently proposed Josephson charge-qubit QC [21], for which a one-qubit rotation takes about 0.1 ns and the corresponding one-qubit coupling is $B_0^{x/z} = 1\epsilon$ in the unit of $\epsilon = 200$ mK. The one-qubit rotations can be controlled by varying the gate voltage for rotations along the z-direction, and by either the applied external magnetic flux through a common inductance or the applied local flux for rotations along the x-direction. The implementation of a two-qubit gate is rather involved and takes about ten times longer than the typical switching time of a one-qubit gate. The corresponding two-qubit coupling is $J_x = 0.05\epsilon$. One of the advantages of this design [21] is that any two charge-qubit in a circuit can be effectively coupled via a common superconducting inductance. Details of the experimental procedure to implement one- and two-qubit gates for this QC proposal can be found in [21]. More general information on Josephson QCs can also be found in a recent review [19]. Throughout our calculations we keep the temperature constant at $\beta = 4\epsilon$, which is within the characteristic low temperature regime ~ 50 mK for Josephson QC proposals [19–21].

In previous studies [7–11] of decoherence, where chaos-generating two-qubit intra-bath interactions have been shown to suppress decoherence, one-body interactions are kept constant and the reduction of decoherence in a subsystem state is monitored via increasing the magnitude of two-body intra-bath interactions. Here we follow a similar approach. However, our interest is in a non-chaotic bath regime. To generate a fast environmental dynamics, we increase the magnitude of $\hat{\sigma}_x$-type one-body intra-bath interactions until they dominate the bath dynamics, i.e. $B_i^x \gg B_i^z$ while keeping the interactions of B_i^z-type fixed. We found nothing special about using strong $\hat{\sigma}_x$-type one-body intra-bath interactions to generate fast environmental dynamics, which we confirmed via increasing the magnitude of $\hat{\sigma}_z$-type intra-bath interactions to achieve $B_i^z \gg B_i^x$ while keeping B_i^x-type interactions fixed. Hence, we considered two different bath configurations. For our first bath configuration, we set $B_c^z = 1\epsilon$ and $B_c^x = 1, 2, 3, 4\epsilon$. Similarly, we set $B_c^x = 1\epsilon$ and $B_c^z = 1, 2, 3, 4\epsilon$ for our second bath configuration. Here, we only present our results for the first bath configuration as a generic representation of our data.

Throughout our study we keep the system–bath coupling and two-body intra-bath couplings constant at $\lambda = J_x = 0.05\epsilon$, which corresponds to the experimentally accessible value of two-qubit interaction strength for the charge-qubit QC [21]. By using the above parameters, we obtained the exact bath eigenenergies and eigenvectors by a Lanczos algorithm [22] for $N = 10$ bath qubits. The numerical solution of the Schrödinger equation for the bipartite states $|\Psi_n(t)\rangle$ is achieved by an 8th order variable stepsize Runge–Kutta method [23]. Time is in the unit of $\hbar/\epsilon = 0.038$ ns.

3. Open system dynamics quantifiers

3.1. Purity and covariance

We aim to show that the strong one-body environmental interactions suppress internal qubit decoherence. In order to monitor the manifestation of this effect, we use two quantities: purity to quantify the extent of decoherence in the subsystem and covariance function to quantify the total magnitude of SEE [24]. We calculate the purity for both the EDD and ID, separately, and by the help of the covariance function we determine the major source of decoherence.

The purity is obtained by tracing over the squared reduced density operator, i.e.

$$\mathcal{P}(t) = \mathrm{Tr}_S\{\hat{\rho}_S^2(t)\}. \tag{20}$$

In the absence of system–environment interactions, the ideal value of purity is unity for pure initial system states. In the presence of system and environment interactions, when subsystem dynamics is non-unitary, the purity gives values less than unity.

To quantify SEE, and thus to verify the presence of the attendant EID, we first calculate the following covariance function [24]:

$$\mathcal{C}_n(t) = \mathrm{Tr}\{\hat{\sigma}_{x/z}^{(0)}\hat{\Sigma}_{x/z}\hat{\rho}_n(t)\} - \mathrm{Tr}\{\hat{\sigma}_{x/z}^{(0)}\hat{\rho}_n(t)\}\,\mathrm{Tr}\{\hat{\Sigma}_{x/z}\hat{\rho}_n(t)\}, \tag{21}$$

for each populated pure state component $|n\rangle$ of the canonical bath state $\hat{\rho}_B(0)$. Here, the averages, given by a full trace $\mathrm{Tr}\{\cdot\}$, are calculated for the bipartite states $\hat{\rho}_n(t) = \hat{U}(t)\hat{\rho}_n(0)\hat{U}^\dagger(t)$ which evolve from the initial conditions of product form $\hat{\rho}_n(0) = \hat{\rho}_S(0) \otimes |n\rangle\langle n|$. By using $\mathcal{C}^n(t)$, we then obtain the absolute value of canonical covariance

$$\mathcal{C}(t) = \sum_{n=1}^{M} p_n|\mathcal{C}_n(t)|. \tag{22}$$

$\mathcal{C}_n(t)$ takes non-vanishing negative values as well as positive values for each $|n\rangle$. The higher the magnitude of $\mathcal{C}_n(t)$ the stronger the SEE and so is the magnitude of EID. To monitor the suppression of EID in a systematic manner, we monitor the time evolution of the absolute value of canonical covariance rather than the canonical covariance itself. Hereafter we simply refer to $\mathcal{C}(t)$ as the covariance. When we systematically increase the magnitude of intra-bath interactions, we expect the covariance function to approach zero in the same manner, indicating the reduction of EID.

3.2. Fidelity and Loschmidt echo

In order to monitor effects of environment-induced unitary shifts on subsystem dynamics, and to analyze these shifts as the magnitude of one-body intra-bath interactions changes, we use fidelity. Purity is not a good error quantifier in this respect. This is because purity, like entropy, is invariant under unitary transformations, and thus is insensitive to environment-induced unitary effects. Fidelity, on the other hand, is sensitive to all sources of environment-induced effects. Hence, a large magnitude of deviation between fidelity and purity decay behavior is a good indicator of unitary shifts emerging in open system dynamics.

Given the free system evolution as

$$\hat{\rho}_S^{\mathrm{free}}(t) = \exp\{-(\mathrm{i}/\hbar)\hat{H}_S t\}\hat{\rho}_S(0)\exp\{(\mathrm{i}/\hbar)\hat{H}_S t\}, \tag{23}$$

the fidelity is defined as an overlap between the free and open system evolutions:

$$\mathcal{F}(t) = \mathrm{Tr}_S\{\hat{\rho}_S(t)\hat{\rho}_S^{\mathrm{free}}(t)\}. \tag{24}$$

The ideal value of fidelity is unity for pure initial states. In the course of open system evolution, whether it is non-unitary or unitary, the fidelity takes values less than unity, reflecting the deviations from the ideal system evolution.

To gain further insight into open system dynamics we also refer to the theory of Loschmidt echo. Recent investigations [25] showed that the Loschmidt echo is a good indicator of the stability of a quantum motion under perturbations and a great deal of information regarding an open system evolution can also be obtained from the Loschmidt echo dynamics [25]. Below, we shortly review the Loschmidt echo formulation of open system dynamics and show the equivalence of Loschmidt echo and fidelity when incoherence dynamics is the only source of decoherence for a quantum subsystem.

When system–environment interactions are not in effect, i.e. $\hat{S}\hat{B} = 0$, dynamics of a bipartite quantum system, composed of a subsystem and and its environment, evolves unitarily $\hat{U}_0(t) = \exp\{-(\mathrm{i}/\hbar)\hat{H}_0(t)\}$ under the Hamiltonian $\hat{H}_0 = \hat{H}_S + \hat{H}_B$, which defines the *unperturbed* time evolution. The *perturbed* time evolution $\hat{U}(t) = \exp\{-(\mathrm{i}/\hbar)\hat{H}t\}$ that emerges as a result of system–environment interactions $\hat{V} = \hat{S}\hat{B}$ is governed by $\hat{H} = \hat{H}_0 + \hat{V}$, which is nothing but the total Hamiltonian (1). When the matter of interest is only the dynamics of a subsystem (or its environment), the perturbed time evolution of the subsystem (or its environment) is non-unitary in general as long as $\hat{V}$ generates non-local quantum correlations between the system and environment degrees of freedom. Nonetheless, under special circumstances, such as when a subsystem (or its environment) evolves in a decoherence-free subspace, a purely unitary subsystem (or environment) evolution is also possible in the presence of perturbations. Depending on the type of perturbation and initial states, non-unitary dynamics may be caused by SEE or the incoherence process alone, or both. Here our interest is in the time evolution of Loschmidt echo when ID is the only source of decoherence for a quantum subsystem, in other words, when the perturbations do not generate any SEE. In such an instance, it turns out that while the environment evolves in a decoherence-free fashion, i.e. unitarily, the subsystem dynamics is non-unitary, provided that the basis states spanning the decoherence-free environment is non-degenerate [12].

For the most, if not all, system–environment models, an appropriate choice of initial state of an environment is of a Gibbsian form, and therefore our focus is on the canonical Loschmidt echo

$$\mathcal{M}(t) = \sum_{n=1}^{M} p_n |f_n(t)|^2, \tag{25}$$

which can conveniently be expressed in terms of the echo amplitudes [25]

$$f_n(t) = \langle \Psi_n(0)|\hat{U}_0(t)\hat{U}(t)|\Psi_n(0)\rangle, \tag{26}$$

where the initial states are of the form $|\Psi_n(0)\rangle = |\psi(0)\rangle \otimes |n\rangle$.

Based on the theory of the Loschmidt echo [25], one can expect a fast environmental dynamics to be more stable against perturbations, which is, for example, a well-established result for chaotic environmental dynamics [25]. Nevertheless, a similar consideration also holds for non-chaotic environmental dynamics. The stabilized quantum motion implies the isolation of environment degree of freedom from the rest of the bipartite system, i.e.

$$\hat{U}(t)|\psi(0)\rangle \otimes |n\rangle = \hat{U}_S^n(t)|\psi(0)\rangle \otimes \hat{U}_B(t)|n\rangle, \tag{27}$$

where $\hat{U}_S^n(t) = \exp\{-(\mathrm{i}/\hbar)\hat{H}_S^n t\}$ defines the perturbed time evolution in the subsystem degree of freedom. As discussed in detail in [12], equation (27) defines a condition for decoherence-free environment evolution under which SEE cannot be generated, i.e. $\mathcal{C}(t) = 0$. This condition is exactly satisfied when $[\hat{H}_B, \hat{B}] = 0$ since $\hat{\rho}_B(0)$ is a function of $\hat{H}_B$. It has been shown by a number of test examples that the above equality is also approximately satisfied when $\hat{C}(t) \to 0$ even though $[\hat{H}_B, \hat{B}] \neq 0$ [12]. Now, since the unperturbed quantum evolution takes the form

$$\hat{U}_0(t)|\psi(0)\rangle \otimes |n\rangle = \hat{U}_S(t)|\psi(0)\rangle \otimes \hat{U}_B(t)|n\rangle, \tag{28}$$

by substituting $\hat{U}_0(t)$ and $\hat{U}(t)$ into equation (26), one can show that the fidelity of the subsystem degree of freedom exactly coincides with the Loschmidt echo of the bipartite system, i.e. $\mathcal{M}(t) = \mathcal{F}(t)$ when the incoherence dynamics is the only source of decoherence. We will use this interesting observation to explain the suppression of the decoherence effect in our study.

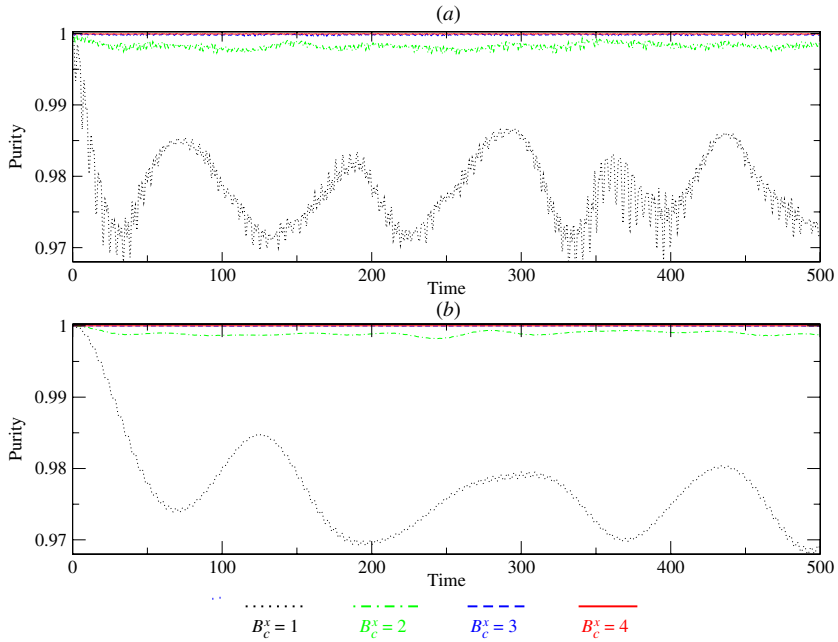

Figure 1. Time evolution of purity $\mathcal{P}(t)$ in the case of xx-type coupling for increasing values of intra-bath interactions, i.e. $B_c^z = 1\epsilon$ and $B_c^x = 1, 2, 3, 4\epsilon$. (*a*) Exact decoherence dynamics and (*b*) incoherence dynamics.

4. Results

In this section, we present our exact numerical and Kraus decomposition results for the open system dynamics quantifiers and analyze the decoherence dynamics of the central qubit for xx- and zz-type couplings and for increasing magnitude of intra-bath interactions, i.e. $B_c^z = 1\epsilon$ and $B_c^x = 1, 2, 3, 4\epsilon$. We plot the time evolution of purity $\mathcal{P}(t)$ in figure 1 for xx-type coupling and in figure 2 for zz-type coupling. In figures 1(*a*) and 2(*a*), we plot the $\mathcal{P}(t)$ for the EDD, obtained by equation (10), and in figures 1(*b*) and 2(*b*), we plot the $\mathcal{P}(t)$ for the ID, predicted by the Kraus decomposition (15).

Both the EDD and ID $\mathcal{P}(t)$ plots show that increasing the magnitude of B_c^x-type intra-bath interaction results in a systematic improvement in $\mathcal{P}(t)$ for both xx- and zz-type couplings. The largest magnitude of decoherence (i.e. the EID as well as the IID) is observed for $B_c^x = 1\epsilon$. A dramatic decrease in $\mathcal{P}(t)$ is seen for $B_c^x = 2\epsilon$, above which the improvement in $\mathcal{P}(t)$ gradually continues, and by the time $B_c^x = 4\epsilon$, the $\mathcal{P}(t)$ is below the theoretically allowed value of 0.999 99 [26].

The EDD $\mathcal{P}(t)$ plots reflect somewhat stronger decoherence than those seen in the ID $\mathcal{P}(t)$ plots. This should not be surprising because the EDD consists of two different mechanisms destroying the qubit coherence, i.e. the SEE and incoherence processes. These two processes cause two different time scales of decoherence: one with high amplitude recurrences originating from the incoherence process, and the other with low amplitude/high frequency oscillations due to the SEE. For both types of couplings, as the B_c^x increases, the IID is suppressed and high amplitude recurrences disappear. Similarly, as the B_c^x increases, the EID is suppressed and low amplitude/high frequency oscillations subside. While these oscillations

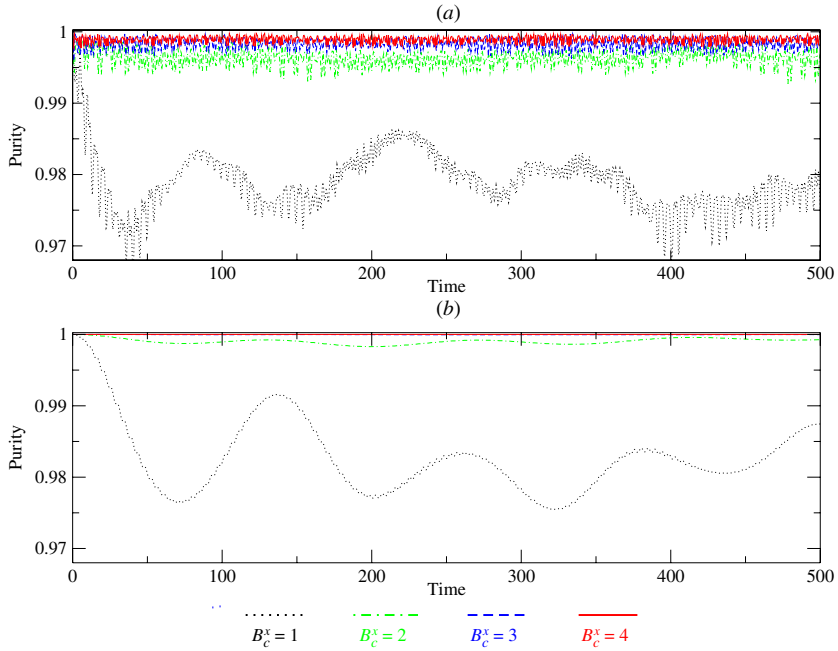

Figure 2. Time evolution of purity $\mathcal{P}(t)$ in the case of zz-type coupling for increasing values of intra-bath interactions, i.e. $B_c^z = 1\epsilon$ and $B_c^x = 1, 2, 3, 4\epsilon$. (*a*) Exact decoherence dynamics and (*b*) incoherence dynamics.

almost completely vanish for xx-type coupling, they do survive for zz-type coupling for which the suppression of EID is slower. For both types of coupling, a comparison between the EDD and ID $\mathcal{P}(t)$ plots show that decoherence is of a comparable order of magnitude for the same value of B_c^x, which indicates that the incoherence process, rather than the SEE, is the major source of internal decoherence.

In figure 3, we plot the time evolution of covariance $\mathcal{C}(t)$ for both xx and zz-type couplings in order to monitor the reduction of SEE. Since the Kraus decomposition of incoherence (12) assumes vanishing SEE, i.e. $\mathcal{C}(t) = 0$, the $\mathcal{C}(t)$ only gives an indication of the suppression of EID. For both types of couplings, the magnitude of $\mathcal{C}(t)$ is systematically reduced as B_c^x increases. Hence, the faster the internal bath dynamics the lower the magnitude of decoherence in the subsystem. While both types of coupling show a decrease in $\mathcal{C}(t)$, the reduction behavior of $\mathcal{C}(t)$ for xx-type coupling is qualitatively different from that of zz-type coupling, especially above $B_c^x \geqslant 2\epsilon$, where we see a systematically and quickly decreasing $\mathcal{C}(t)$ with increasing B_c^x. However, in the case of zz-type coupling, the reduction behavior of $\mathcal{C}(t)$ is slow and small in magnitude, and thus slightly stronger decoherence is observed for zz-type coupling cases than that seen for xx-type coupling.

We plot the time evolution of fidelity $\mathcal{F}(t)$ and Loschmidt echo $\mathcal{M}(t)$ in figures 4 and 5 for xx- and zz-type couplings, respectively, for increasing values of the intra-bath interactions, i.e. $B_c^z = 1\epsilon$ and $B_c^x = 1, 2, 3, 4\epsilon$. The $\mathcal{F}(t)$ is plotted for the EDD in figures 4(*a*) and 5(*a*), and for the ID in figures 4(*b*) and 5(*b*). The exact time evolution of $\mathcal{M}(t)$ is plotted in figures 4(*c*) and 5(*c*).

For the smallest value of intra-bath interactions, i.e. $B_c^x = 1\epsilon$, where the worst decoherence is observed, the EDD $\mathcal{F}(t)$ and $\mathcal{M}(t)$ plots show large magnitude highly irregular oscillations

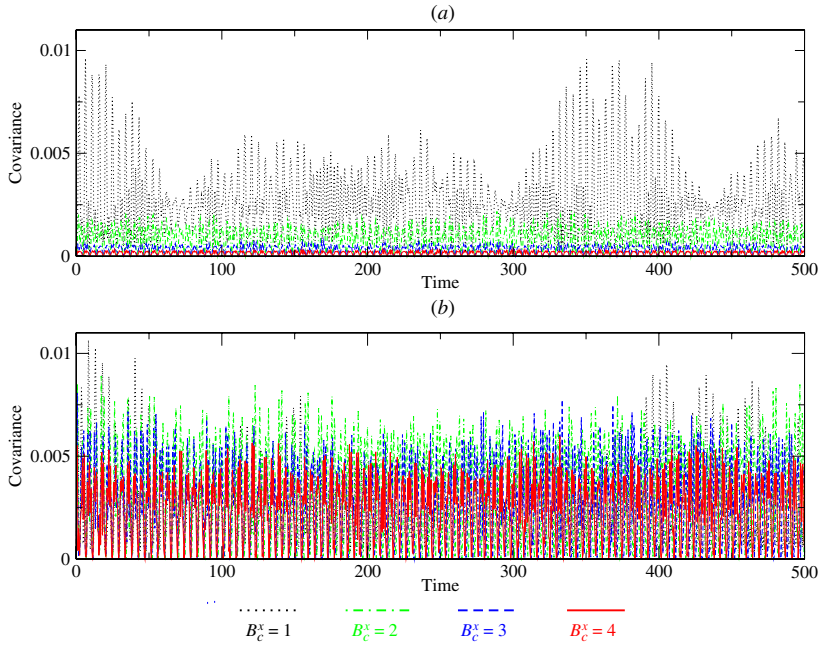

Figure 3. Time evolution of covariance $\mathcal{C}(t)$ for increasing values of intra-bath interactions, i.e. $B_c^z = 1\epsilon$ and $B_c^x = 1, 2, 3, 4\epsilon$. (*a*) xx-type coupling and (*b*) zz-type coupling.

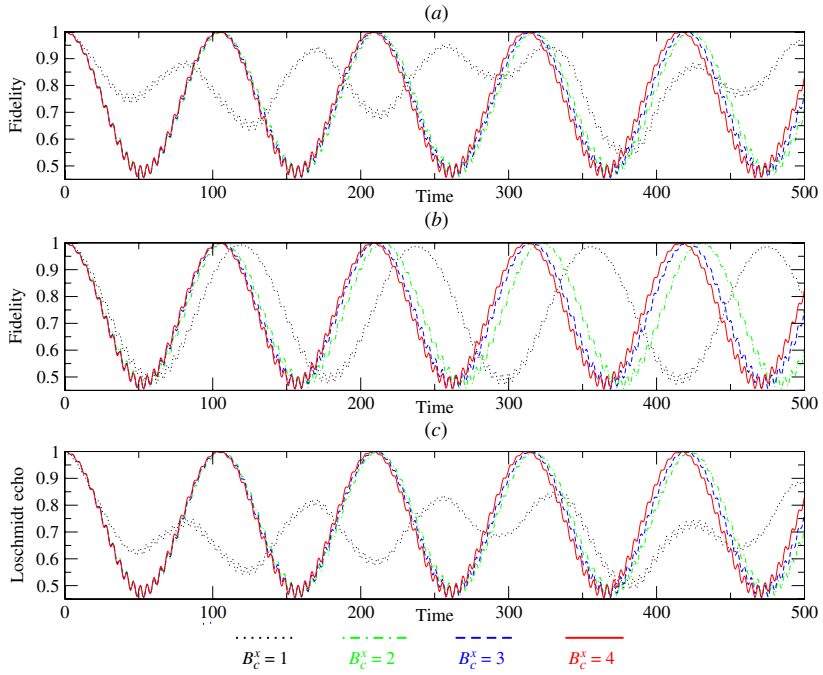

Figure 4. Time evolution of fidelity $\mathcal{F}(t)$ and Loschmidt echo $\mathcal{M}(t)$ in the case of xx-type coupling for increasing values of intra-bath interactions, i.e. $B_c^z = 1\epsilon$ and $B_c^x = 1, 2, 3, 4\epsilon$. (*a*) Exact decoherence dynamics of $\mathcal{F}(t)$, (*b*) incoherence dynamics of $\mathcal{F}(t)$ and (*c*) exact dynamics of $\mathcal{M}(t)$.

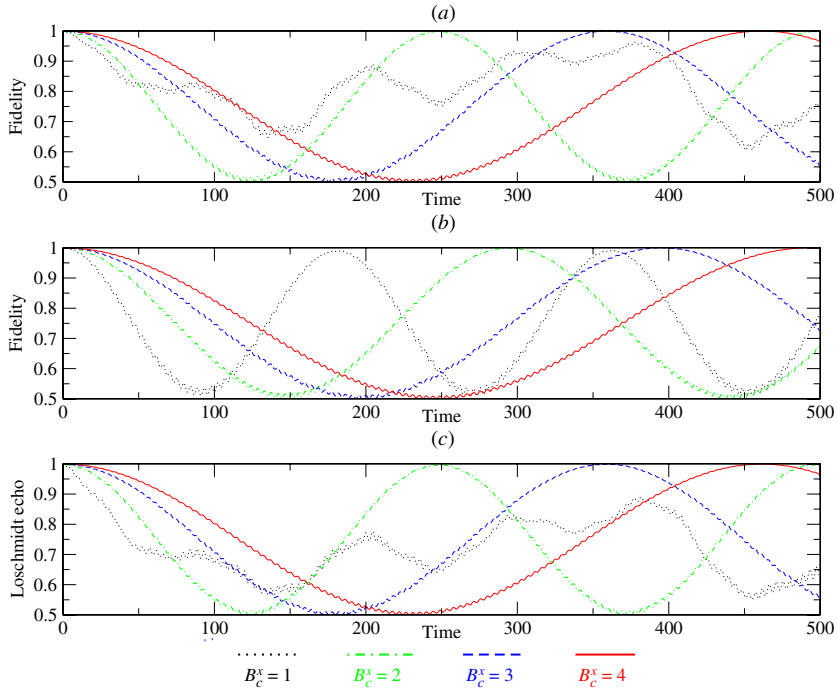

Figure 5. Time evolution of fidelity $\mathcal{F}(t)$ and Loschmidt echo $\mathcal{M}(t)$ in the case of zz-type coupling for increasing values of intra-bath interactions, i.e. $B_c^z = 1\epsilon$ and $B_c^x = 1, 2, 3, 4\epsilon$. (*a*) Exact decoherence dynamics of $\mathcal{F}(t)$, (*b*) incoherence dynamics of $\mathcal{F}(t)$ and (*c*) exact dynamics of $\mathcal{M}(t)$.

for both types of coupling. This irregular behavior is due to the SEE, and therefore not observed for the ID $\mathcal{F}(t)$ plots, the dynamical behavior of which follows a regular periodic pattern. For the greater values of intra-bath interactions, i.e. $B_c^x \geqslant 2\epsilon$, the decoherence is of a negligible extent, and the environment-induced coherent shifts emerge as the only dominant effect. As a result, the EDD and ID $\mathcal{F}(t)$ plots exactly overlap. This is because ID becomes exact when SEE is vanishing. Moreover, as shown in section 3.2 and seen in figures 4 and 5, the $\mathcal{F}(t)$ and $\mathcal{M}(t)$ plots exactly overlap for the absolute ID, which again occurs in the absence of SEE.

The periodic behavior of $\mathcal{F}(t)$ and $\mathcal{M}(t)$ for $B_c^x \geqslant 2\epsilon$ does not correlate with the $\mathcal{P}(t)$ decay behavior at all. The periodic $\mathcal{F}(t)$ and $\mathcal{M}(t)$ oscillations also display a high sensitivity to the changes in B_c^x for zz-type coupling but almost no such sensitivity is seen for xx-type coupling. Moreover, the magnitude of deviation of $\mathcal{F}(t)$ and $\mathcal{M}(t)$ from the ideal system evolution is enormous in all cases, which was not indicated by the $\mathcal{P}(t)$ plots even for $B_c^x = 1\epsilon$. These large deviations from the ideal system evolution are due to the environment-induced unitary effects. The $\mathcal{P}(t)$ plots did not show any apparent indication of these unitary effects. This is because the $\mathcal{P}(t)$, like entropy, is invariant under unitary transformations, and thus cannot detect unitary effects. On the other hand, the $\mathcal{F}(t)$ as well as $\mathcal{M}(t)$ is sensitive to both non-unitary and unitary effects. Therefore, the tandem use of $\mathcal{P}(t)$ and $\mathcal{F}(t)$ or $\mathcal{M}(t)$ in the characterization of open system dynamics supplies more valuable information than when either of these error quantifiers was used alone.

5. Discussions

In this section, we discuss a number of effects observed in our study. In doing so, we discuss non-unitary and unitary effects separately.

5.1. Non-unitary effects

Two major mechanisms are responsible for the observed decoherence suppression in our study: fast environmental dynamics, which causes the suppression of EID, and a rapid decrease in the number of populated bath states, which not only leads to an immediate reduction of IID but also contributes to the suppression of EID.

The suppression of EID by a fast environmental dynamics can be explained by the Loschmidt echo formulation of open system evolution, in which system–environment interactions are treated as perturbations acting on both system and environment degrees of freedom. The Loschmidt echo measures the stability of a quantum motion against perturbations. In our study we monitored the dynamical changes in our subsystem as the magnitude of one-body intra-bath interactions increases. We observed that the fast environmental dynamics causes a systematic reduction of SEE and eventually leads on to a complete suppression of EID. Once a quantum subsystem is free of EID, the incoherence process, governed by the Kraus decomposition (12), emerges as the only source of decoherence. As a result, the fidelity of the subsystem exactly coincides with the Loschmidt echo of a bipartite system, i.e. a subsystem plus its environment. This is only possible when the dynamics of an environment is isolated from the rest of the bipartite system. However, since we do not simply have $\hat{S}\hat{B} = 0$, the isolation is then only possible if the dynamics of an environment evolves in a decoherence-free fashion with respect to the subsystem [12]. Hence, the role of the fast environmental dynamics is to generate (at least effectively) a decoherence-free environment condition, under which SEE cannot be formed, and thus EID can be avoided [12]. This should not be surprising because SEE is a correlation transfer process, in the course of which states of a quantum subsystem and its environment are correlated non-locally so that the total entangled state of such a bipartite system cannot be written as a product state of its components. Hence, provided that the dynamics of an environment evolves decoherence freely, the formation of SEE and thus the resulting EID in the subsystem degree of freedom can be avoided [12].

The effectiveness of a decoherence-free time evolution depends on the condition-generating decoherence-free subspace [12]. For example, if a bath Hamiltonian and a bath-coupling operator are related by a natural symmetry, e.g. they form a family of commutative operators, this would be an exact condition for a decoherence-free environment [12]. However, in the absence of such an apparent symmetry, the decoherence suppression may manifest quiet differently for different types of couplings, as indicated by covariance plots, which showed that the suppression of EID is faster for xx-type coupling cases than those of zz-type coupling. Since we obtained the fast environmental dynamics by increasing the magnitude of B_c^x-type interactions to achieve $B_i^x \gg B_i^z$ for each bath qubit i, our bath Hamiltonian $\hat{H}_B$ was dominated by $\hat{\sigma}_x$-type operators. This suggests that $[\hat{H}_B, \hat{\Sigma}_x] \to 0$ and thus $\mathcal{C}(t) \to 0$ as $B_i^x \gg B_i^z$. However, in the case of zz-type coupling, we obtained $\mathcal{C}(t) \to 0$ but also, by the same token, $[\hat{H}_B, \hat{\Sigma}_z] \neq 0$ since $[\hat{\Sigma}_x, \hat{\Sigma}_z] \neq 0$. Hence, the faster suppression of decoherence for xx-type coupling is due to the similarity between the eigenstates of $\hat{H}_B$ and $\hat{\Sigma}_x$. And, since these eigenstates are orthogonal, they lead to vanishingly small off-diagonal matrix elements $b^{m,n} \simeq 0$ that are responsible for the formation of SEE. However, since the zz-type coupling cases do not have such an extra symmetry contribution, we observed a slower suppression of EID and surviving SEE even for $B_c^x = 4\epsilon$.

The second effect responsible for the decoherence suppression is the rapid decrease in the number of populated bath states as a consequence of increasing the energy gap between the ground and first excited states of the bath spectrum as the magnitude of one-body intra-bath interactions increases. Due to the very low relevant bath temperature for the charge-qubit QC [21], even for $B_c^x = 1\epsilon$, the population of the 12th excited state is already on the order of $p_{12} = 10^{-5}$. For $B_c^x = 2\epsilon$, we have $p_8 = 10^{-5}$, which is responsible for the abrupt improvement seen in the purity plots, see figures 1 and 2. For $B_c^x = 3\epsilon$ and $B_c^x = 4\epsilon$, the population of the first excited state is on the order of $p_2 = 10^{-5}$ and $p_2 = 10^{-7}$, respectively, for which the magnitude of decoherence was of a negligible extent. This is because the only populated bath state effective in decoherence of the central qubit is the ground state. Hence, the environmental dynamics not only evolves in a decoherence-free fashion but also in adiabatic-like given by equation (13). Due to the decoherence-free and adiabatic-like evolution, non-chaotic baths with fast internal dynamics can be superior to chaotic baths [7–11] as decoherence suppressors for several reasons that we briefly discuss below.

While the chaos-generating strong two-body interactions have been shown to be very effective in reducing decoherence in certain instances [7–11], the experimental implementation of such strong interactions in a QC core may not be practical within today's technological limits. For example, a typical two-qubit gate span for the charge-qubit QC [21] on which our study based is ten times longer than that of a one-qubit gate, which means that the corresponding two-body coupling strength for a two-qubit gate is ten times smaller in magnitude than that of a one-qubit gate. Whereas an effective suppression of decoherence in order to keep the purity within theoretically acceptable limit of 0.999 99 [26] requires one- and two-body coupling strengths to be at least of the same order of magnitude [7–9]. Hence, deliberately induced chaotic interactions in a QC core may not be a feasible approach, at least in the near future, to avoid decoherence. Therefore, an alternative way of tackling internal decoherence issue, which may or may not accompany the chaos approach, can be very useful. Our results suggest that strong one-body intra-bath interactions also very effectively reduce decoherence, and thus can be used to correct non-unitary type errors. Moreover, there should always exist a low temperature regime so that fast environmental dynamics evolves adiabatically from its ground state and thus incoherence process can be avoided. However, for a chaotic bath, the density of bath states would be high, and therefore, even though EID is completely suppressed by a chaotic bath, IID may emerge as a more serious source of error than EID.

5.2. *Unitary effects*

The suppression of decoherence is of interesting consequences for open system dynamics quantifiers which are sensitive to both non-unitary and unitary effects. As a result of suppression of non-unitary effects, i.e. both EID and IID, we have seen that the fidelity and Loschmidt echo plots display a completely periodic behavior. This periodic behavior emerges from the environment-induced unitary shift. Even though non-unitary effects induced by an environment can be completely suppressed, unitary effects may not be avoided. The shift, even though unitary, may be a serious impediment to the performance of quantum gates since any deviation from the ideal system evolution, whether non-unitary or unitary in nature, is an error source.

Below, by assuming that incoherence process is the only source of decoherence, i.e. SEE is negligibly small, we derive an explicit formula for the fidelity and examine the dynamical behavior of this error quantifier. In the absence of system–environment interactions, the ideal subsystem evolution (23) beats with the frequency $\omega_0 = \beta_0/2\hbar$ where $\beta_0 = \left(B_x^2 + B_z^2\right)^{1/2}$. The system–environment interactions perturb the ideal system evolution for each populated

pure state component $|n\rangle$ of the canonical bath state $\hat{\rho}_B(0)$, resulting in the shifted subsystem frequencies $\omega^n_{x/z} = \beta^n_{x/z}/2\hbar$ where $\beta^n_{x/z}$ are given by equations (17) and (19).

By using equations (15), (23) and (24), the fidelity of incoherence dynamics can be expressed as

$$\mathcal{F}(t) = \sum_{n=1}^{M} (p_n/8)\big\{\gamma_1 \cos 2\omega^n_{x/z} t + \gamma_2 \cos 2\big(\omega^n_{x/z} - \omega_0\big)t + 2(\gamma_3 + \gamma_4 \cos 2\omega_0 t) + \gamma_5 \cos 2\big(\omega^n_{x/z} + \omega_0\big)t\big\}, \tag{29}$$

where the coefficients $\gamma_1, \gamma_2, \gamma_3, \gamma_4$ and γ_5 depend on three parameters:

$$\gamma_1 = -2(-1 + c^2 - d^2 + e^2), \qquad \gamma_2 = (1 + c - d - e)(1 + c + d + e),$$
$$\gamma_3 = 1 + c^2 + d^2 + e^2, \qquad \gamma_4 = 1 - c^2 - d^2 + e^2, \qquad \gamma_5 = (-1 + c + d - e)(-1 + c - d + e)$$

which are

$$c = \big(B^{z\,2}_0 + B^x_0 B^n_x\big)\big/\big(\beta_0 \beta^n_x\big), \qquad d = B^x_0/\beta_0, \qquad e = B^n_x/\beta^n_x \tag{30}$$

for xx-type coupling and

$$c = \big(B^{x\,2}_0 + B^z_0 B^n_z\big)\big/\big(\beta_0 \beta^n_z\big), \qquad d = B^x_0/\beta_0, \qquad e = B^x_0/\beta^n_z \tag{31}$$

for zz-type coupling. To simplify the above fidelity equation, recall that $B^{x/z}_0 = 1\epsilon$ for the central qubit. Since the magnitude of system–bath interactions are relatively weak $\lambda_i \simeq 0.05\epsilon$, we can assume that $c \simeq 1$ and $d = 1/\sqrt{2} \simeq e$. Moreover, since we are interested in the low temperature regime, where the only ground state of bath is effectively populated, i.e. $p_{n=1} \simeq 1$, we reach a simplified equation for the fidelity

$$\mathcal{F}(t) = \tfrac{1}{4}\big[3 + \cos 2\big(\omega^{n=1}_{x/z} - \omega_0\big)t\big], \tag{32}$$

which can reproduce the observed periodic behavior for $B^x_c \geqslant 2\epsilon$. Hence, the observed periodic fidelity dynamics emerges from the shift terms $b^{n=1}_{x/z}$, and the period of the observed oscillations is given by $P^{n=1}_{x/z} = \pi\big/\big(\omega_0 - \omega^{n=1}_{x/z}\big)$. Also, $\mathcal{F}(t)$ can be approximated for very low temperatures by substituting $b^{n=1}_{x/z}$ with the canonical averages of the bath coupling operator $\bar{\Sigma}_{x/z} = \mathrm{Tr}_B\{\hat{\Sigma}_{x/z}\hat{\rho}_B(0)\}$.

We have seen that the period of fidelity oscillations is highly sensitive to the changes in the magnitude of intra-bath interactions for zz-type coupling but almost no sensitivity is observed for xx-type coupling. This different dynamical behavior of fidelity for different couplings is directly related to the changes in the diagonal matrix elements of the bath coupling operator as the strength of intra-bath interactions increases. In figure 6, the diagonal matrix element of the bath coupling operator, i.e. $b^{n=1}_{x/z}$, calculated for the ground state of the bath, i.e. $n = 1$, and the associated periods of fidelity, i.e. $P^{n=1}_{x/z}$, are plotted for increasing values of intra-bath interactions. For xx-type coupling, as B^x_c increases, $b^{n=1}_x$ only slightly increases, and above $B^x_c = 2\epsilon$, the increment is negligibly small. Accordingly, the changes in $P^{n=1}_x$ in response to the changes in $b^{n=1}_x$ are also negligibly small. Hence, the fidelity dynamics is insensitive to the changes in B^x_c for xx-type coupling. However, for zz-type coupling, increasing B^x_c results in a quicker and steady decline of $b^{n=1}_z$, which results in more rapid changes in $P^{n=1}_z$, and thus highly sensitive behavior of fidelity to the changes in B^x_c.

Coherent shifting is an interesting effect originating from the system–environment interactions. However, unlike decoherence or dissipation, the shift affects the system unitarily. Unitary errors generated by the shift may impose a serious limitation on the performance of quantum gates. A quantum algorithm consists of a sequence of large number of elementary qubit gates operating on an input state, in a predetermined order, to reach a target state. An

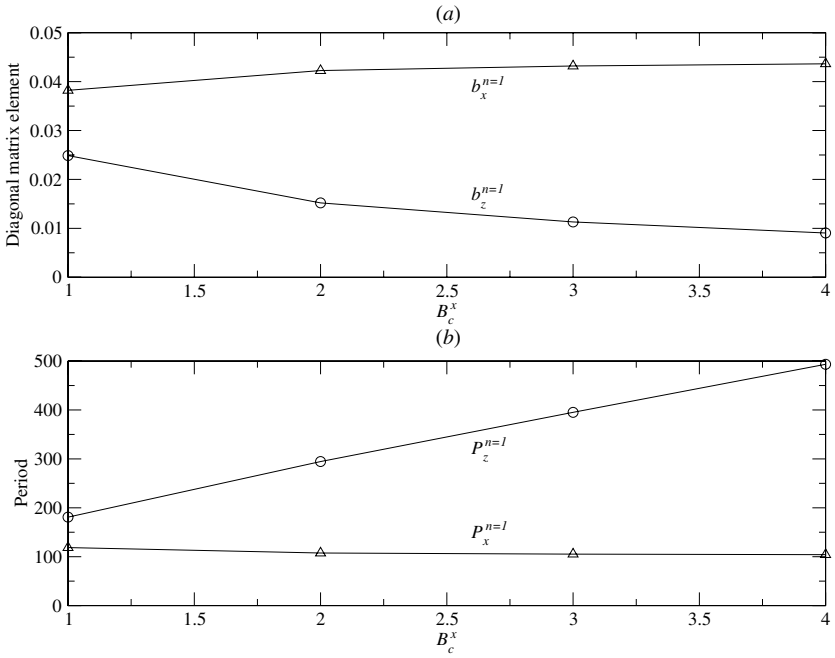

Figure 6. (*a*) Diagonal matrix element of bath coupling operators $b_{x/z}^{n=1}$ and (*b*) the associated period of fidelity $P_{x/z}^{n=1}$ plotted as a function of B_c^x. Data points are connected by lines to guide the eye.

output state after an elementary gate in the sequence is an input state for the subsequent gate. Once a gate is infected by a coherent shift, the attendant error spreads over the other gates and grows in time quickly as the number of elementary gates increases, eventually rendering the outcome of computation unpredictable. This means that the retroactive error correction is not guaranteed, and thus error correction protocols should operate in parallel with elementary gate components, which at best, considerably overloads the computational task. To avoid such deleterious unitary errors in a QC core, prior knowledge of coherent shifting, i.e. the type and magnitude of the shift, can extremely be advantageous in designing effective error correction strategies to calibrate quantum gates against the shift, especially for architecture-dependent intrinsic errors.

6. Summary

Residual qubit–qubit interactions emerging in a many-qubit QC core generate an inevitable internal decoherence mechanisms for the ideal computational states of qubits. Therefore, even though decoherence time imposed by an external environment surrounding a QC core is infinite, an efficient operation of a QC is not guaranteed in the presence of residual qubit–qubit interactions. By using the open system dynamics quantifiers, i.e. purity, covariance, fidelity and Loschmidt echo, we analyzed the exact internal decoherence dynamics of a qubit within an isolated QC in the presence of one- and two-body static internal imperfections. Our analysis enabled us to distinguish between non-unitary and unitary components of open system dynamics and to show that two non-unitary processes, i.e. system–environment entanglement

and incoherence are responsible for the internal qubit decoherence. We found that the major source of internal decoherence is induced by the incoherence process rather than system–environment entanglement. Furthermore, we showed that fast environmental dynamics results in a rapid reduction of decoherence induced by both system–environment entanglement and incoherence processes. We explained the mechanisms of suppression of decoherence for these two processes and discussed our results.

Acknowledgments

The author acknowledges the financial support provided by the Department of Chemistry, Simon Fraser University. Special thanks go to N Çetinbaş for carefully reading the manuscript.

References

[1] Joos E, Zeh H D, Kiefer C, Giulini D, Kupsch J and Stamatescu I-O 2003 *Decoherence and the Appearance of a Classical World in Quantum Theory* (New York: Springer)
[2] Breuer H-P and Petruccione F 2003 *The Theory of Open Quantum Systems* (New York: Oxford University Press)
[3] Gardiner C W and Zoller P 2004 *Quantum Noise* 3rd edn (Berlin: Springer)
[4] Nielsen M A and Chuang I L 2000 *Quantum Computation and Quantum Information* (Cambridge: Cambridge University Press)
[5] See e.g. Brown K R, Harrow A W and Chuang I L 2004 *Phys. Rev.* A **70** 052318
[6] Georgeot B and Shepelyansky D L 2000 *Phys. Rev.* E **62** 3504
Georgeot B and Shepelyansky D L 2000 *Phys. Rev.* E **62** 6366
Georgeot B and Shepelyansky D L 1998 *Phys. Rev. Lett.* **81** 5129
Benenti G, Casati G and Shepelyansky D L 2001 *Eur. Phys. J.* D **17** 265
Montangero S, Benenti G and Fazio R 2003 *Phys. Rev. Lett.* **91** 187901
[7] Çetinbaş M and Wilkie J 2007 *Phys. Lett.* A **370** 207
[8] Çetinbaş M and Wilkie J 2008 *J. Phys. A: Math. Theor.* **41** 065302
[9] Çetinbaş M and Wilkie J 2007 *Phys. Lett.* A **370** 194
[10] Çetinbaş M and Wilkie J 2008 *Phys. Lett.* A **372** 990
Çetinbaş M and Wilkie J 2008 *Phys. Lett.* A **372** 1194
[11] See e.g. Olsen F F, Olaya-Castro A and Johnson N F 2007 *J. Phys.: Conf. Ser.* **84** 012006
Pineda C, Gorin T and Seligman T H 2007 *New J. Phys.* **9** 106
Yuan X Z, Goan H-S and Zhu K-D 2007 *New J. Phys.* **9** 219
Relano A, Dukelsky J and Molina R A 2007 *Phys. Rev.* E **76** 046223
Gorin T, Pineda C and Seligman T H 2007 *Phys. Rev. Lett.* **99** 240405
Jun Jing and Hong-Ru Ma 2007 *Chin. Phys.* **16** 1489
Rossini D, Calarco T, Giovannetti V, Montangero S and Fazio R 2007 *J. Phys. A: Math. Theor.* **40** 8033
Rossini D, Calarco T, Giovannetti V, Montangero S and Fazio R 2007 *Phys. Rev.* A **75** 032333
Olaya-Castro A, Lee C F and Johnson N F 2006 *Europhys. Lett.* **74** 208
Ma X S, Wang A M, Yang X D and You H 2005 *J. Phys. A: Math. Gen.* **38** 2761
Yuan X Z and Zhu K D 2005 *Europhys. Lett.* **69** 868
Yuan X Z, Zhu K D and Wu Z J 2005 *Eur. Phys. J.* D **33** 129
Lucamarini M, Paganelli S and Mancini S 2004 *Phys. Rev.* A **69** 062308
Alicki R 2004 *Open Sys. Inf. Dyn.* **11** 53
Žnidarič M and Prosen T 2003 *J. Phys. A: Math. Gen.* **36** 2463
Tessieri L and Wilkie J 2003 *J. Phys. A: Math. Gen.* **36** 12305
Paganelli P, de Pasquale F and Giampaolo S M 2002 *Phys. Rev.* A **66** 052317
Prosen T and Seligman T H 2002 *J. Phys. A: Math. Gen.* **35** 4707
Dawson C M, Hines A P, McKenzie R H and Milburn G J 2005 *Phys. Rev.* A **71** 052321
[12] Çetinbaş M 2009 *J. Phys. A: Math. Theor.* **42** 145302
[13] Zanardi P and Rasetti M 1997 *Mod. Phys. Lett.* B **11** 1085

[14] Lidar D A and Whaley K B 2003 Decoherence-free subspaces and subsystems *Irreversible Quantum Dynamics (Springer Lecture Notes in Physics* vol 622*)* ed F Benatti and R Floreanini (Berlin: Springer) pp 83–120 Also at quant-ph/0301032
[15] Lidar D A, Bacon D and Whaley K B 1999 *Phys. Rev. Lett.* **82** 4556
[16] Zurek W H 1981 *Phys. Rev.* D **24** 1516
Zurek W H 1982 *Phys. Rev.* D **26** 1862
Zurek W H 2003 *Rev. Mod. Phys.* **75** 715
[17] Kraus K 1971 *Ann. Phys., NY* **64** 311
Kraus K 1983 *States, Effects and Operations: Fundamental Notions of Quantum Theory* (Berlin: Springer)
[18] Prokof'ev N V and Stamp P C E 2000 *Rep. Prog. Phys.* **63** 669
[19] Makhlin Y, Schön G and Shnirman A 2001 *Rev. Mod. Phys.* **73** 357 and references therein
[20] Nakamura Y *et al* 1999 *Nature (Lond)* **398** 786
Martinis J M, Nam S and Aumentado J 2002 *Phys. Rev. Lett.* **89** 117901
Vion D *et al* 2002 *Science* **296** 886
Yu Y *et al* 2002 *Science* **296** 889
Chiorescu I *et al* 2003 *Science* **299** 1869
Simmonds R W *et al* 2004 *Phys. Rev. Lett.* **93** 077003
[21] You J Q, Tsai J S and Nori F 2002 *Phys. Rev. Lett.* **89** 197902
[22] Lehoucq R B, Sorensen D C and Yang C 1998 *ARPACK Users' Guide: Solution of Large-Scale Eigenvalue Problems with Implicitly Restarted Arnoldi Methods* (Philadelphia, PA: SIAM)
[23] Hairer E, Norsett S P and Wanner G 1993 *Solving Ordinary Differential Equations: I. Nonstiff Problems (Springer Series in Computational Mathematics* vol 8*)* 2nd edn (Berlin: Springer)
[24] Davis R I A, Delbourgo R and Jarvis P D 2000 *J. Phys. A: Math. Gen.* **33** 1895
[25] Gorin T, Prosen T, Seligman T H and Žnidarič M 2006 *Phys. Rep.* **435** 33
Prosen T and Žnidarič M 2003 *New J. Phys.* **5** 109 and references therein
[26] Loss D and DiVincenzo D-P 1998 *Phys. Rev.* A **57** 120